Metal–Metal Bonds

DOI: 10.1002/ange.201102296

Theory-Guided Experiments on the Mechanistic Elucidation of the Reduction of Dinuclear Zinc, Manganese, and Cadmium Complexes**

*Duan-Yen Lu, Jen-Shiang K. Yu, Ting-Shen Kuo, Gene-Hsiang Lee, Yu Wang, and Yi-Chou Tsai**

Since the recognition of the first Zn^{I}–Zn^{I} bond in the dinuclear sandwich decamethyldizincocene $[(\eta^5\text{-}C_5Me_5)Zn–Zn(\eta^5\text{-}C_5Me_5)]$,[1] the chemistry of Zn–Zn-bonded species has grown so rapidly that many complexes of the type LZn–ZnL have been characterized and studied.[2] Regardless of the denticity of the supporting ligands L, they all coordinate to Zn in a terminally chelating mode.[2] However, formation of these dinuclear compounds has not been mechanistically examined. We recently described the characterization of dinuclear Zn^{I}–Zn^{I}-bonded species $[\{\kappa^2\text{-}Me_2Si(NDipp)_2\}Zn–Zn\{\kappa^2\text{-}Me_2Si(NDipp)_2\}]^{2-}$ (**2**) (Dipp = 2,6-*i*$Pr_2C_6H_3$) from KC_8 reduction of dinuclear zinc complex $[Zn_2(\mu\text{-}\kappa^2\text{-}Me_2Si(NDipp)_2)_2]$ (**1**), whereby the coordination mode of the diamido ligands dramatically changes from bridging to chelating.[2j] We thus became interested in the structural preference and the formation mechanism of Zn^{I}–Zn^{I}-bonded complexes. Elaborate calculations were performed to understand the reduction of **1**, and a plausible mechanism was then proposed (Scheme 1). On two-electron reduction of **1**, two intermediates, **Ia** and **Ib**, are generated, and the energy difference between them is only 0.3 kcal mol^{-1}.[2j] The Zn^{II}–Zn^{I}-bonded mixed-valent intermediate **Ia** is produced by one-electron reduction of **1**, and subsequently undergoes a dramatic structural rearrangement to give **Ib**, in which one three-coordinate and one one-coordinate Zn atoms are proposed. The exact valence of the Zn atoms in **Ib** is still not clear.

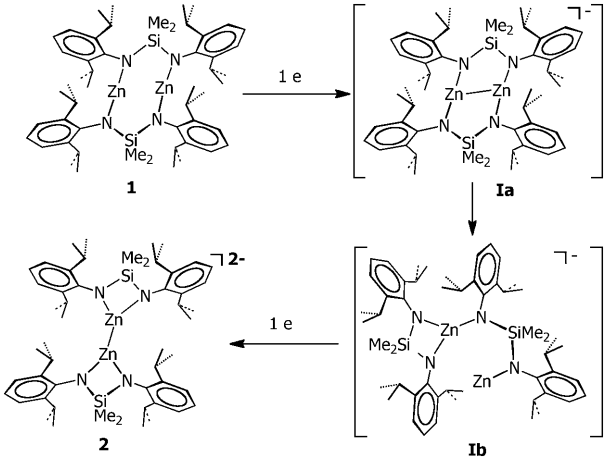

Scheme 1. Calculated mechanism of transformation of **1** into **2**.

Although the application of quantum chemical methods (ab initio molecular orbital and density functional theory) to elucidate reaction mechanisms has been very successful,[3] most of the time it is difficult to prove the theoretically developed reaction mechanisms by experiments. This is indeed the case for the transformation from **1** to **2**. Attempts to probe both intermediates **Ia** and **Ib** failed. To this end, we turned our attention from zinc to manganese and cadmium, because they not only show structural similarity in the reported M^{I}–M^{I}-bonded dinuclear complexes $[(\kappa^2\text{-Nacnac})M–M(\kappa^2\text{-Nacnac})]$ (M = Zn,[2o] Mn;[4] Nacnac = $HC[C(Me)NDipp]_2$) and [Ar′M–MAr′] (M = Zn,[2n] Cd;[5] Ar′ = 2,6-(2,6-*i*$Pr_2C_6H_3)_2C_6H_3$), but also feature an identical M–M σ-bonding scheme. Herein we report structural transformations on reduction of dinuclear manganese and cadmium complexes $[Mn_2\{\kappa^2\text{-}Me_2Si(NDipp)_2\}_2]$ (**3**) and $[Cd_2\{\mu\text{-}\kappa^2\text{-}Me_2Si(NDipp)_2\}_2]$ (**4**). Characterization of the products supports the computed mechanism shown in Scheme 1.

As shown in Scheme 2, reactions of the dilithiated diamido ligand and 1 equiv of anhydrous $MnCl_2$ and $CdCl_2$ in diethyl ether and THF, respectively, yielded the corresponding dimeric compounds **3** and **4** in good yields. The dinuclear nature of **3** and **4** was deciphered by single-crystal X-ray crystallography,[6] and their molecular structures are provided in Figures S1 and S2 of the Supporting Information. Complex **3** is essentially composed of two MnN_2Si four-membered rings, which are brought together by two Mn–N bonds, and consequently exhibit a boat conformation with two manganese atoms at the stern and two Si atoms at the bow. Each Mn atom is embraced by three nitrogen atoms and adopts a distorted T-shaped geometry. The central Mn_2N_2

[*] D.-Y. Lu, Prof. Dr. Y.-C. Tsai
Department of Chemistry, National Tsing Hua University
Hsinchu 30013 (Taiwan)
Fax: (+886) 3-571-1082
E-mail: yictsai@mx.nthu.edu.tw
Prof. Dr. J.-S. K. Yu
Institute of Bioinformatics and Systems Biology and Department of Biological Science and Technology, National Chiao Tung University
Hsinchu, 30010 (Taiwan)
T.-S. Kuo
Department of Chemistry, National Taiwan Normal University
Taipei 11677 (Taiwan)
Dr. G.-H. Lee, Prof. Dr. Y. Wang
Department of Chemistry, National Taiwan University
Taipei 10617 (Taiwan)

[**] J.-S.K.Y. and Y.-C.T are indebted to the National Science Council, Taiwan for support under Grant NSC 99-2627-B-009-008 and NSC 99-2113-M-007-012-MY3, respectively. The computational facility is supported by NCTU under the grant from MoE ATU Plan. We thank Prof. Yen-Hsiang Liu (Fu Jen Catholic University, Taiwan) for his help with the crystallography of compound **6**.

Supporting information for this article (experimental details for the synthesis and characterization of complexes **3**–**7**) is available on the WWW under http://dx.doi.org/10.1002/anie.201102296.

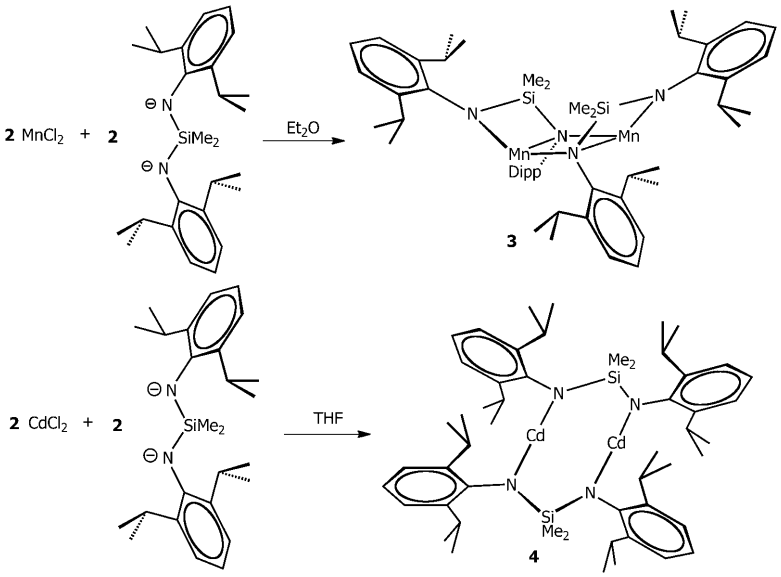

Scheme 2.

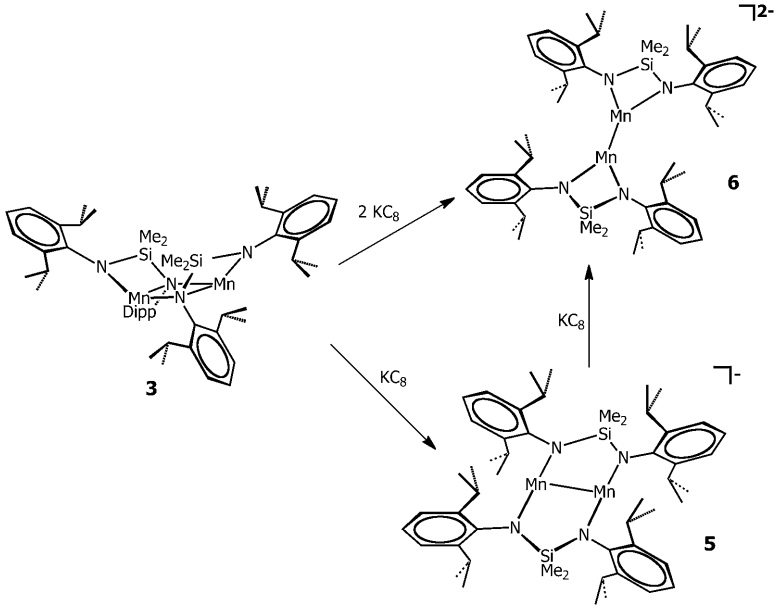

Scheme 3.

four-membered ring adopts a nonplanar conformation, with a dihedral angle of 11.0°. Presumably, this arrangement is a consequence of strain between the sterically encumbered Dipp substituents. A similar bonding mode was also observed in complexes $[M_2\{\kappa^2\text{-}N(Dipp)(CH_2)_3(Dipp)N\}_2]$ (M = Mn, Fe, and Zn).[7]

The Mn···Mn distance of 2.7746(11) Å in **3** is significantly longer than that of 2.69 Å in $[M_2\{\kappa^2\text{-}N(Dipp)(CH_2)_3(Dipp)N\}_2]$[7] but shorter than those of $[Mn_2\{N(SiMe_3)_2\}_4]$ (2.811(1) Å at 140 K[8a] and 2.841(1) at room temperature[8b]). Solid-state magnetic data of **3** are shown in Figure S3 of the Supporting Information. Variation of χ_m and μ_{eff} with temperature indicates antiferromagnetic coupling between two manganese centers. The μ_{eff} value of 4.88 μ_B at 300 K is significantly lower than the spin-only value ($S = 5/2$ for dinuclear manganese species).

Complex **4**, on the other hand, is essentially isostructural with complex **1**,[2j] whereby two metal atoms are spanned by two bidentate diamido ligands, and the Cd···Cd distance of 3.042(1) Å indicates no bonding interaction between the two cadmium atoms.

Both **3** and **4** show interesting reduction chemistry. Whereas **2** is the only isolable product from the reduction of **1**, the reduction of complex **3** is slightly more complicated. As shown in Scheme 3, treatment of **3** with 1 equiv of KC_8 in the presence of 18-crown-6 in THF afforded orange mixed-valent Mn^{II}–Mn^{I} complex $[(thf)_2K\subset 18\text{-crown-}6][Mn_2\{\mu\text{-}\kappa^2\text{-}Me_2Si(NDipp)_2\}_2]$ ($[(thf)_2K\subset 18\text{-crown-}6][\mathbf{5}]$). Subsequent reduction of $[(thf)_2K\subset 18\text{-crown-}6][\mathbf{5}]$ gave purple Mn^{I}–Mn^{I} species $[(thf)_2K\subset 18\text{-crown-}6]_2[Mn\{\kappa^2\text{-}Me_2Si(NDipp)_2\}_2]$ ($[(thf)_2K\subset 18\text{-crown-}6]_2[\mathbf{6}]$). Alternatively, dianionic complex **6** can be prepared directly from **3** by two-electron reduction. For crystallographic experiments, two more complexes containing dianionic fragment **6** were prepared by KC_8 reduction of **3** in neat toluene and in THF in the presence of 222-cryptand to give $[K_2\subset\mathbf{6}]$ and $[K\subset 222\text{-cryptand}]_2[\mathbf{6}]$, respectively.

The solid-state molecular structure of anionic **5** was determined by single crystal X-ray crystallography (Figure 1).[6] The structure of **5** is close to that of calculated intermediate **Ia**; both feature two bidentate diamido ligands spanning an M^{II}–M^{I} (M = Mn, Zn) bond. In contrast to the planar Mo_2N_4 core in quadruply bonded dimolybdenum complex $[Mo_2\{\mu\text{-}\kappa^2\text{-}Me_2Si(NDipp)_2\}_2]$,[9] in which two bidentate diamido ligands also span the Mo–Mo bond, the core structure of **5** displays a puckered conformation with an N1-Mn1-Mn2-N2 dihedral angle of 24.3°. Each Mn atom is ligated by two nitrogen donors of the ligands and one adjacent Mn atom, and thus adopts a T-shaped geometry. Although **5** is a mixed-valent ($Mn^{II}Mn^{I}$) species, the two Mn atoms are essentially indistinguishable, because the structure has local C_i symmetry. Characterization of **5** therefore supports the accuracy of the calculated intermediate **Ia** for the reduction of **1**.

Surprisingly, the X-ray structure of dianionic complex **6** in both $[K\subset 222\text{-cryptand}]_2[\mathbf{6}]$ and $[K_2\subset\mathbf{6}]$ (Figure 2) is dramatically different from that of **5**, but similar to that of **2**. In both compounds, each Mn atom is terminally chelated by two bidentate diamido ligands, and the two resultant MnN_2Si four-membered rings are brought together by the Mn–Mn bond. In **6**, each Mn atom is three-coordinate with respect to the diamido ligand and the neighboring Mn atom, and adopts a trigonal-planar geometry with a sum of the bond angles at each Mn center of 360°. Noteworthily, the two MnN_2Si four-

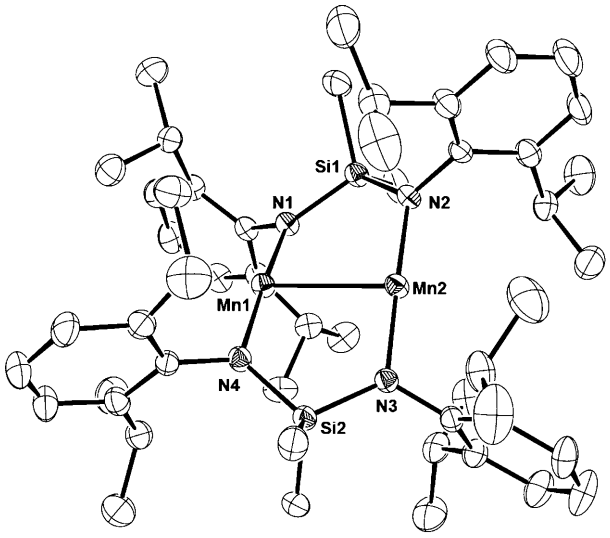

Figure 1. Molecular structure of **5** with thermal ellipsoids at 35% probability. Selected bond lengths [Å] and angles [°]: Mn1–Mn2 2.6848(8), Mn1–N1 1.934(3), Mn1–N4 1.940(3), Mn2–N2 1.941(3), Mn2–N3 1.937(3); N1-Mn1-N4 173.99(13), N2-Mn2-N3 177.09(13), N1-Mn1-Mn2 88.56(9), N4-Mn1-Mn2 91.26(9), N3-Mn2-Mn1 89.52(9), N2-Mn2-Mn1 91.14(9).

membered rings are coplanar in both complexes regardless of the encapsulated potassium ions. This array is in sharp contrast with that of [(κ^2-Nacnac)Mn–Mn(κ^2-Nacnac)], in which two C_3N_2Mn six-membered rings are orthogonal to each other.[4]

Not only do monoanionic **5** and dianionic **6** exhibit different structures, but they have very different metrics according to XRD analysis. The average Mn–N bond lengths are 1.939 (**5**), 2.054 ([K_2⊂**6**]), and 2.089 Å ([K⊂222-cryptand]$_2$[**6**]). The significantly short Mn–N bond lengths in **5** suggest significant π-bonding interactions between manganese atoms and four nitrogen donors. For a dinuclear complex, the metal–metal distance is usually the most interesting metric parameter. The Mn–Mn bond length of 2.6851(9) Å in **5** is much shorter than those in [K⊂222-cryptand]$_2$[**6**] (2.7871(8) Å) and [K_2⊂**6**] (2.7464(13) Å). Interestingly, the Mn–Mn bond length is strongly dependent on the ancillary ligands. For example, the Mn–Mn bond lengths in univalent dimanganese species are 2.721(1) Å in [(κ^2-Nacnac)Mn–Mn(κ^2-Nacnac)][4] and 2.6745(5) Å in [Mn_2(μ-S_2)(CO)$_6$(μ-CO)].[10] In addition, the Mn–Mn bond length in zero-valent dimanganese carbonyl complex [Mn_2(CO)$_{10}$] is 2.9042(8) Å.[11] Nevertheless, all of these values are shorter than those of diatomic Mn_2 (3.4 Å, estimated in rare-gas matrix) and Mn_2^+ (3.06 Å, estimated in MgO matrix).[12] Roesky et al. have shown that the Mn^I–Mn^I bond in [(κ^2-Nacnac)Mn–Mn(κ^2-Nacnac)][4] is formed by overlap of a pair of 4s orbitals. Accordingly, a similar bonding scheme is also proposed for the Mn–Mn bonds in **5** and **6**, but the formal Mn–Mn bond order is 0.5 in **5** and 1 in **6**. The shorter Mn–Mn bond length in **5** is presumably due to the bridging ligands, while **6** bears two chelating ligands.

It is noteworthy that the two ZnN_2Si four-membered rings in the reported dinuclear Zn^I–Zn^I-bonded complex [Zn{κ^2-

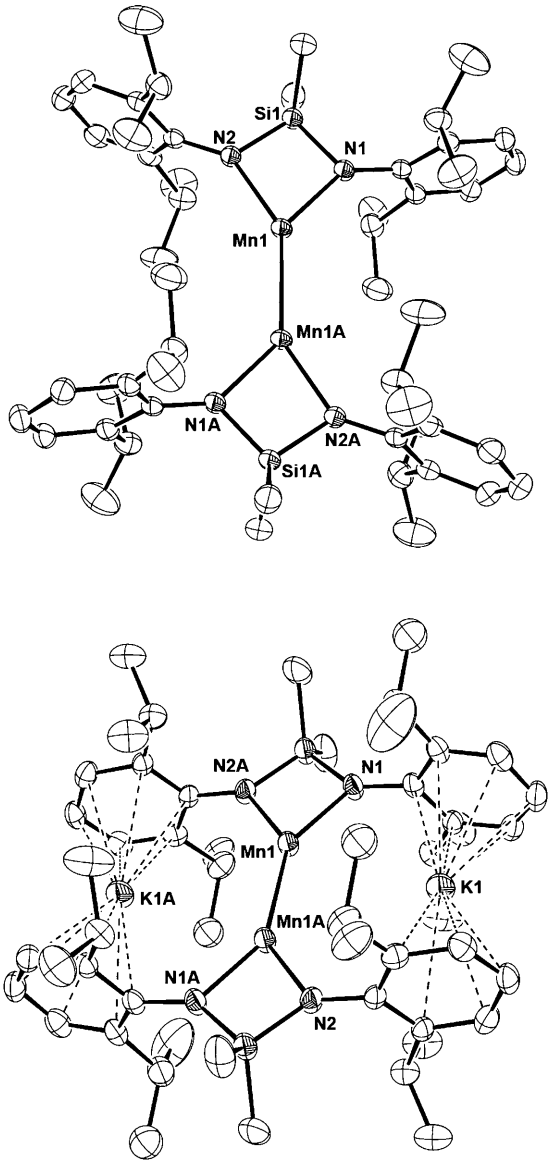

Figure 2. Molecular structures of **6** in [K⊂222-cryptand]$_2$[**6**] (top) and [K_2⊂**6**] (bottom) with thermal ellipsoids at 35% probability. Selected bond lengths [Å] and angles [°]: [K⊂222-cryptand]$_2$[**6**]: Mn1–Mn1A 2.7871(8), Mn1–N1 2.078(3), Mn1–N2 2.100(2); N1-Mn1-N2 76.44(10), N1-Mn1-Mn1A-N2A 11.69(10). [K_2⊂**6**]: Mn1–Mn1A 2.7464(13), Mn1–N1 2.065(4), Mn1–N2 2.044(4), Mn1···K1 3.8731(14); N1-Mn1-N2 76.74(15), N1-Mn1-Mn1A-N2 4.02(12).

$Me_2Si(NDipp)_2$}]$_2^{2-}$ (**2**)[2j] are not coplanar and display a dihedral angle of 50.6°. The Zn–Zn σ-bonding character was further corroborated by characterization of K_2⊂**2**, in which each potassium atom is sandwiched by two adjacent phenyl rings of Dipp groups, and consequently the dihedral angle of the two N_2SiZn four-membered rings is reduced to 10.8°. The steady Zn–Zn distances of 2.3695(17) and 2.3634(11) Å in these two complexes, independent of rotation about the Zn–Zn axis, indeed signify σ bonding between the two Zn atoms. On the other hand, in light of the Mn–Mn σ-bonding scheme in [(κ^2-Nacnac)Mn–Mn(κ^2-Nacnac)],[4] both [K_2⊂**6**] and [K⊂222-cryptand]$_2$[**6**] should also have a Mn–Mn σ bond on the basis of equivalent Mn–Mn distances. However, the

parallel arrangement of two MnN_2Si four-membered rings in both [K⊂222-cryptand]$_2$[**6**] and [K_2⊂**6**] suggests strong antiferromagnetic coupling between two Mn centers. This is indeed the case. The temperature dependence of the magnetic susceptibility of mixed-valent dimanganese $Mn^{II}Mn^{I}$ species [$(thf)_2$K⊂18-crown-6][**5**] and univalent Mn^{I}–Mn^{I} complex [K_2⊂**6**] in the temperature range of 2–300 K is shown in Figures S4 and S5 of the Supporting Information, respectively. The room-temperature effective magnetic moments μ_{eff} of [$(thf)_2$K⊂18-crown-6][**5**] and [K_2⊂**6**] are 6.10 and 4.84 μ_B, respectively. These values are smaller than that expected for two noninteracting univalent manganese centers ($\mu_{eff} = 9.8$ μ_B for ^{7}S and $\mu_{eff} = 6.9$ μ_B for ^{5}D states).

To isolate the **5**-analogous dicadmium complex, reduction of **4** by 1 equiv of potassium hydride in the presence of 18-crown-6 was also carried out in THF. To our surprise, a diamagnetic tetranuclear mixed-valent complex formulated as [$(thf)_2$K⊂18-crown-6]$_2$[({κ^2-Me_2Si(NDipp)$_2$}Cd{μ-Me_2Si(NDipp)$_2$}Cd)$_2$] ([$(thf)_2$K⊂18-crown-6]$_2$[**7**]) was obtained from the reaction (Scheme 4). Two signals at $\delta = 436.0$ and 420.3 ppm were observed in the ^{113}Cd NMR spectrum. In contrast to the high stability of the only structurally characterized Cd^{I}–Cd^{I}-bonded dimeric species [Ar′Cd–CdAr′] (Ar′ = 2,6-(2,6-*i*$Pr_2C_6H_3$)$_2C_6H_3$), [$(thf)_2$K⊂18-crown-6]$_2$[**7**] is thermally unstable in organic solvents. On dissolution in THF at room temperature, it quickly decomposes to cadmium metal, free ligands, and unidentified cadmium complexes over 12 h. X-ray diffraction analysis of **7** (Figure 3) indicates that it is a dimeric complex in which two monomers {(κ^2-Me_2Si(NDipp)$_2$)Cd(μ-Me_2Si(NDipp)$_2$)Cd}, containing one one-coordinate and one three-coordinate Cd atoms, are linked through a Cd^{I}–Cd^{I} bond. The structure of this monomer is identical to that of calculated dizinc intermediate **Ib** in Scheme 1. It is therefore clear that the one-coordinate zinc atom in **Ib** is univalent, and the three-coordinate zinc atom is divalent. The Cd1–Cd1A bond length of 2.6103(9) Å is shorter than that in Ar′Cd–CdAr′ (2.6257(5) Å),[5] in which both cadmium atoms are also mono-coordinate with respect to the aryl ligand. Presumably, owing to the smaller size of Mn and Zn atoms, the **7**-analogous dimanganese and dizinc complexes have not yet been observed.

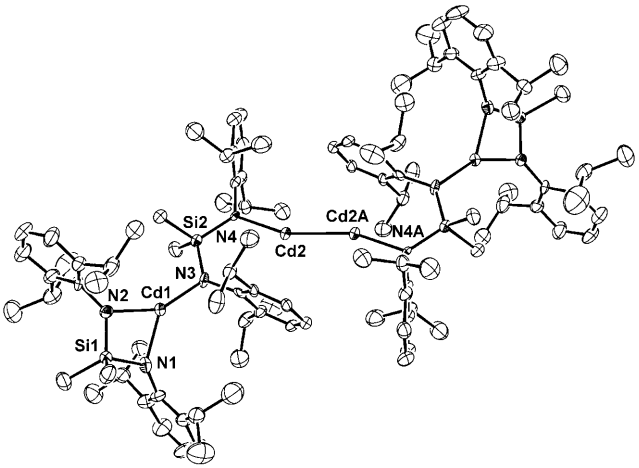

Figure 3. Molecular structure of **7** with thermal ellipsoids at 35% probability. Selected bond lengths [Å] and angles [°]: Cd1–Cd1A 2.6103(9), Cd1–N1 2.103(5), Cd2–N2 2.111(5), Cd2–N3 2.183(6), Cd2–N4 2.169(5); N1-Cd1-Cd1A 158.24(15), N2-Cd2-N3 139.54(19), N2-Cd2-N4 147.7(2), N3-Cd2-N4 72.3(2).

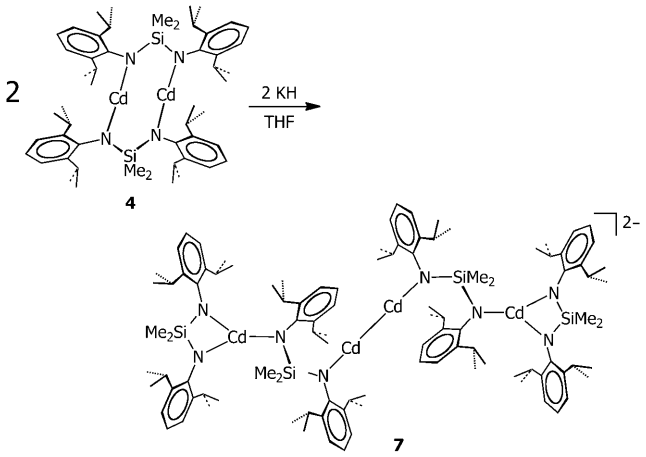

Scheme 4.

In summary, we have demonstrated the synthesis and characterization of two remarkable Mn–Mn-bonded dimanganese complexes, **5** and **6**, and one tetracadmium complex **7** featuring a Cd^{I}–Cd^{I} bond. Collectively, characterization of these complexes is consistent with the proposed intermediates in the computed mechanism for the transformation of dizinc complex **1** on reduction, and this mechanism is applicable to the reduction of dimanganese complex **3** and dicadmium complex **4**. Although the recently reported dinuclear complexes LM–ML (M = Zn,[2] Mn,[4] Cd[5]) can be stabilized by various ligands with different denticity, the mechanism described herein sheds light on their formation. Reactivity studies on **5**–**7** are currently underway.

Received: April 2, 2011
Published online: June 29, 2011

Keywords: cadmium · manganese · metal–metal interactions · reaction mechanisms · zinc

[1] I. Resa, E. Carmona, E. Gutierrez-Puebla, A. Monge, *Science* **2004**, *305*, 1136.

[2] a) S. Gondzik, D. Bläser, C. Wölper, S. Schulz, *Chem. Eur. J.* **2010**, *16*, 13599; b) M. Carrasco, R. Peloso, A. Rodríguez, E. Álvarez, C. Maya, E. Carmona, *Chem. Eur. J.* **2010**, *16*, 9754; c) S. Schulz, S. Gondzik, D. Schuchmann, U. Westphal, L. Dobrzycki, R. Boese, S. Harder, *Chem. Commun.* **2010**, *46*, 7757; d) Y. Liu, S. Li, X.-J. Yang, P. Yang, J. Gao, Y. Xia, B. Wu, *Organometallics* **2009**, *28*, 5270; e) S. Schulz, D. Schuchmann, I. Krossing, D. Himmel, D. Bläser, R. Boese, *Angew. Chem.* **2009**, *121*, 5859; *Angew. Chem. Int. Ed.* **2009**, *48*, 5748; f) I. L. Fedushkin, O. V. Eremenko, A. A. Skatova, A. V. Piskunov, G. K. Fukin, S. Y. Ketkov, E. Irran, H. Schumann, *Organometallics* **2009**, *28*, 3863; g) S. Schulz, D. Schuchmann, U. Westphal, M. Bolte, *Organometallics* **2009**, *28*, 1590; h) D. Schuchmann, U. Westphal, S. Schulz, U. Florke, D. Bläser, R.

Boese, *Angew. Chem.* **2009**, *121*, 821; *Angew. Chem. Int. Ed.* **2009**, *48*, 807; i) A. Grirrane, I. Resa, A. Rodríguez, E. Carmona, *Coord. Chem. Rev.* **2008**, *252*, 1532; j) Y.-C. Tsai, D.-Y. Lu, Y.-M. Lin, J.-K. Hwang, J.-S. K. Yu, *Chem. Commun.* **2007**, 4125; k) I. L. Fedushkin, A. A. Skatova, S. Y. Ketkov, O. V. Eremenko, A. V. Piskunov, G. K. Fukin, *Angew. Chem.* **2007**, *119*, 4380; *Angew. Chem. Int. Ed.* **2007**, *46*, 4302; l) X.-J. Yang, J. Yu, Y. Liu, Y. Xie, H. F. Schaefer, Y. Liang, B. Wu, *Chem. Commun.* **2007**, 2363; m) A. Grirrane, I. Resa, A. Rodriguez, E. Carmona, E. Álvarez, E. Gutierrez-Puebla, A. Monge, A. Galindo, D. del Rio, R. A. Andersen, *J. Am. Chem. Soc.* **2007**, *129*, 693; n) Z. Zhu, R. J. Wright, M. M. Olmstead, E. Rivard, M. Brynda, P. P. Power, *Angew. Chem.* **2006**, *118*, 5939; *Angew. Chem. Int. Ed.* **2006**, *45*, 5807; o) Y. Wang, B. Quillian, P. Wei, H. Wang, X.-J. Yang, Y. Xie, R. B. King, P. v. R. Schleyer, H. F. Schaefer III, G. H. Robinson, *J. Am. Chem. Soc.* **2005**, *127*, 11944; p) T. M. Greene, W. Brown, L. Andrews, A. J. Downs, G. V. Chertihin, N. Runeberg, P. Pyykkö, *J. Phys. Chem.* **1995**, *99*, 7925.

[3] a) S. Niu, M. B. Hall, *Chem. Rev.* **2000**, *100*, 353; b) K. Koga, K. Morokuma, *Chem. Rev.* **1991**, *91*, 823; c) D. G. Musaev, K. Morokuma in *Advances in Chemical Physics*, Vol. XCV (Eds.: S. A. Rice, I. Prigogine), Wiley, New York, **1996**, p. 61; d) P. E. M. Siegbahn, M. R. A. Blomberg in *Theoretical Aspects of Homogeneous Catalysts, Applications of Ab Initio Molecular Orbital Theory* (Eds.: P. W. N. M. van Leeuwen, J. H. van Lenthe, K. Morokuma), Kluwer Academic Publishers, Hingham, MA, **1995**; e) T. Ziegler, *Chem. Rev.* **1991**, *91*, 651; f) D. R. Salahub, M. Castro, R. Fournier, P. Calaminici, N. Godbout, A. Goursot, C. Jamorski, H. Kobayashi, A. Martinez, I. Papai, E. Proynov, N. Russo, S. Sirois, J. Ushio, A. Vela in *Theoretical and Computational Approaches to Interface Phenomena* (Eds.: H. Sellers, J. Olab), Plenum, New York, **1995**, p. 187; g) P. E. M. Siegbahn in *Advances in Chemical Physics*, Vol. XCIII (Eds.: S. A. Rice, I. Prigogine), Wiley, New York, **1996**, p. 333; h) *Transition Metal Hydrides* (Ed.: A. Dedieu), VCH Publishers, Weinheim, **1992**; i) *Theoretical Aspects of Homogeneous Catalysis, Applications of Ab Initio Molecular Orbital Theory* (Eds.: P. W. N. M. van Leeuwen, J. H. van Lenthe, K. Morokuma), Elsevier, Dordrecht, **1994**; j) S. Yoshida, S. Sakaki, H. Kobayashi, *Electronic Processes in Catalyst*, VCH, New York, **1992**.

[4] J. Chai, H. Zhu, A. C. Stückl, H. W. Roesky, J. Magull, A. Bencini, A. Caneschi, D. Gatteschi, *J. Am. Chem. Soc.* **2005**, *127*, 9201.

[5] Z. Zhu, R. C. Fischer, J. C. Fettinger, E. Rivard, M. Brynda, P. P. Power, *J. Am. Chem. Soc.* **2006**, *128*, 15068.

[6] Crystallographic data for **3**·THF: $C_{56}H_{90}Mn_2N_4O_1Si_2$, $M_r = 1001.38$, $T = 200(2)$ K, orthorhombic, space group *Pccn*, $a = 13.4453(2)$, $b = 17.8769(3)$, $c = 24.0109(5)$ Å, $V = 5771.27(18)$ Å^3, $Z = 4$, $\rho_{calcd} = 1.152$ Mg m^{-3}, $\mu = 0.518$ mm^{-1}, reflections collected: 21690, independent reflections: 5273 ($R_{int} = 0.0602$), final R indices [$I > 2\sigma(I)$]: $R_1 = 0.0730$, $wR_2 = 0.1966$, R indices (all data): $R_1 = 0.1024$, $wR_2 = 0.2261$; **4**: $C_{52}H_{80}Cd_2N_4Si_2$, $M_r = 1042.18$, $T = 200(2)$ K, monoclinic, space group $P2_1/n$, $a = 12.4901(2)$, $b = 18.6490(5)$, $c = 12.7453(3)$ Å, $\beta = 116.3250(10)°$, $V = 2660.86(10)$ Å^3, $Z = 2$, $\rho_{calcd} = 1.301$ Mg m^{-3}, $\mu = 0.880$ mm^{-1}, reflections collected: 13188, independent reflections: 4801 ($R_{int} = 0.0499$), final R indices [$I > 2\sigma(I)$]: $R_1 = 0.0458$, $wR_2 = 0.1155$, R indices (all data): $R_1 = 0.0635$, $wR_2 = 0.1396$; [(thf)$_2$K⊂18-crown-6][**5**]·2THF: $C_{80}H_{136}K_1Mn_2N_4O_{10}Si_2$: $M_r = 1519.09$, $T = 200(2)$ K, monoclinic, space group $P2_1/c$, $a = 17.1441(2)$, $b = 12.5878(2)$, $c = 41.3059(5)$ Å, $\beta = 96.5760(10)°$, $V = 8855.4(2)$ Å^3, $Z = 4$, $\rho_{calcd} = 1.139$ Mg m^{-3}, $\mu = 0.412$ mm^{-1}, reflections collected: 38589, independent reflections: 15930 ($R_{int} = 0.0751$), final R indices [$I > 2\sigma(I)$]: $R_1 = 0.0754$, $wR_2 = 0.2013$, R indices (all data): $R_1 = 0.1191$, $wR_2 = 0.2376$; [K⊂222-cryptand]$_2$[**6**]·2THF: $C_{100}H_{176}K_2Mn_2N_8O_{15}Si_2$: $M_r = 1974.75$, $T = 200(2)$ K, triclinic, space group $P\bar{1}$, $a = 13.9385(9)$, $b = 15.0562(9)$, $c = 17.2750(11)$ Å, $\alpha = 112.6360(10)$, $\beta = 111.3730(10)$, $\gamma = 92.5690(10)°$, $V = 3042.9(3)$ Å^3, $Z = 1$, $\rho_{calcd} = 1.078$ Mg m^{-3}, $\mu = 0.350$ mm^{-1}, reflections collected: 20983, independent reflections: 10374 ($R_{int} = 0.0256$), final R indices [$I > 2\sigma(I)$]: $R_1 = 0.0671$, $wR_2 = 0.2088$, R indices (all data): $R_1 = 0.0864$, $wR_2 = 0.22379$; [K_2⊂**6**]: $C_{52}H_{80}K_2Mn_2N_4Si_2$: $M_r = 1005.46$, $T = 200(2)$ K, monoclinic, space group $P2_1/n$, $a = 10.0750(5)$, $b = 21.3090(12)$, $c = 13.5660(8)$ Å, $\beta = 100.857(5)°$, $V = 2860.3(3)$ Å^3, $Z = 2$, $\rho_{calcd} = 1.167$ Mg m^{-3}, $\mu = 0.663$ mm^{-1}, reflections collected: 12868, independent reflections: 5538 ($R_{int} = 0.0623$), final R indices [$I > 2\sigma(I)$]: $R_1 = 0.0577$, $wR_2 = 0.1642$, R indices (all data): $R_1 = 0.1171$, $wR_2 = 0.2271$; **7**: $C_{165}H_{264}Cd_4K_2N_8O_{16}Si_4$: $M_r = 3256.00$, $T = 150(2)$ K, monoclinic, space group $P2_1/c$, $a = 16.7796(4)$, $b = 25.7323(6)$, $c = 20.6035(5)$ Å, $\beta = 90.3056(11)°$, $V = 8896.0(4)$ Å^3, $Z = 2$, $\rho_{calcd} = 1.216$ Mg m^{-3}, $\mu = 0.602$ mm^{-1}, reflections collected: 40979, independent reflections: 15648 ($R_{int} = 0.0706$), final R indices [$I > 2\sigma(I)$]: $R_1 = 0.0711$, $wR_2 = 0.1924$, R indices (all data): $R_1 = 0.1325$, $wR_2 = 0.2176$. CCDC 818305 (**3**), 818306 (**4**), 818307 ([(thf)$_2$K⊂18-crown-6][**5**]·2THF), 818308 ([K⊂222-cryptand]$_2$[**6**]·2THF) 818309 ([K_2⊂**6**]), and 818310 (**7**) contain the supplementary crystallographic data for this paper. These data can be obtained free of charge from The Cambridge Crystallographic Data Centre via www.ccdc.cam.ac.uk/data_request/cif.

[7] J. Chai, H. Zhu, Q. Ma, H. W. Roesky, H.-G. Schmidt, M. Noltemeyer, *Eur. J. Inorg. Chem.* **2004**, 4807.

[8] a) D. C. Bradley, M. B. Hursthouse, K. M. A. Malik, R. Möseler, *Transition Met. Chem.* **1978**, *3*, 253; b) B. D. Murray, P. P. Power, *Inorg. Chem.* **1984**, *23*, 4584.

[9] Y.-C. Tsai, Y.-M. Lin, J.-S. K. Yu, J.-K. Hwang, *J. Am. Chem. Soc.* **2006**, *128*, 13980.

[10] a) R. D. Adams, O.-S. Kwon, M. D. Smith, *Inorg. Chem.* **2001**, *40*, 5322; b) R. D. Adams, O.-S. Kwon, M. D. Smith, *Inorg. Chem.* **2002**, *41*, 5525.

[11] R. Bianchi, G. Gervasio, D. Marabello, *Inorg. Chem.* **2000**, *39*, 2360.

[12] S. K. Nayak, B. K. Rao, P. Jena, *J. Phys. Condens. Matter* **1998**, *10*, 10863.

